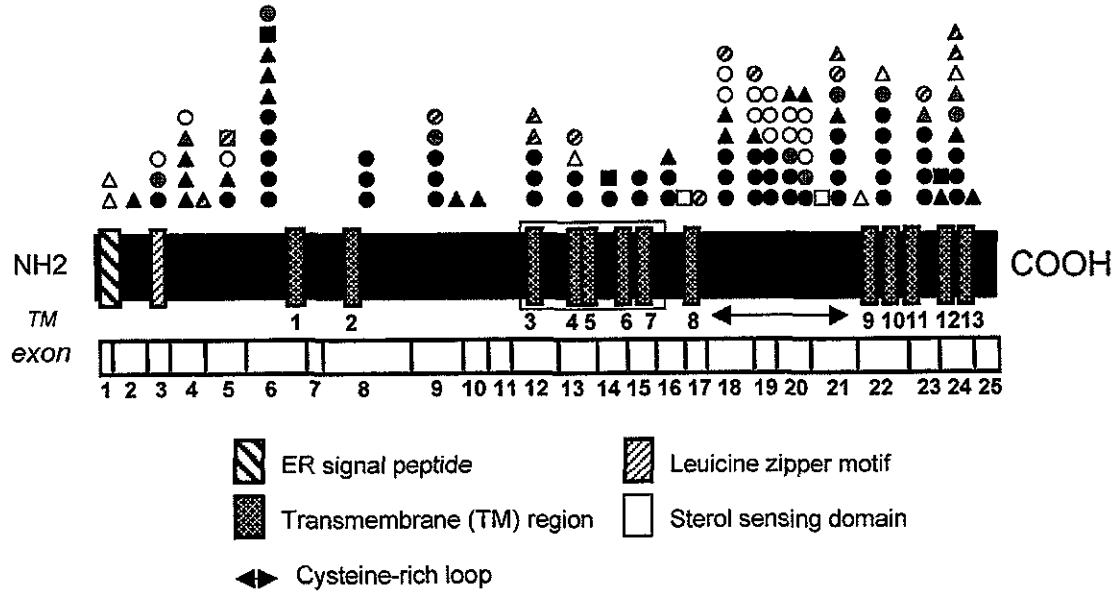


Fig. 1. Schematic representation of the primary structure of *NPC1* in which some special domains are emphasized. TM, transmembrane regions. Exon boundaries are indicated by vertical lines. The reported *NPC1* mutations are depicted as follows: circles indicate missense mutations, triangles indicate frameshift mutations including nonsense mutations, and rectangles indicate in-frame mutations including deletions and insertions. Black spots indicate the severe late infantile type, gray indicates the intermediate *juvenile* type, and white indicates the milder adult type NP-C.

loops, six small cytoplasmic loops, and a short cytoplasmic tail (Figs. 1 and 2) [9,11,12]. The exact function of NPC1 and the role of cholesterol accumulation in the neuropathology of NP-C remain to be defined. Here, we report on our ongoing comprehensive molecular analysis of *NPC1* and describe two novel disease-causing mutations.

## 2. Methods

### 2.1. Patients

NP-C was diagnosed in a total of 13 patients based on filipin staining of skin fibroblasts [1,2]. Clinical features of these patients are summarized in Table 1 [13,14].

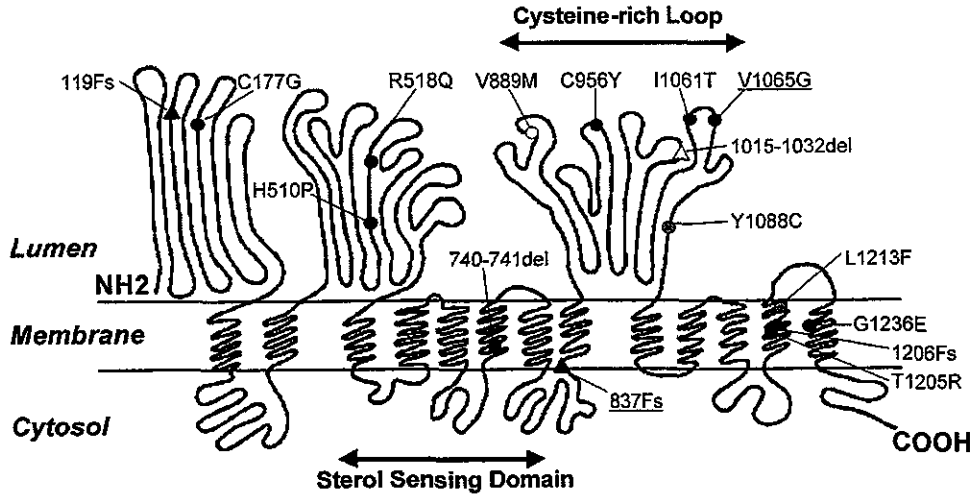


Fig. 2. Localization of *NPC1* mutations. The mutations reported in this study are depicted in the NPC1 protein scheme proposed by Davis and Ioannou (2000) [13]. Circles indicate missense mutations, triangles indicate frameshift mutations including nonsense mutations, and rectangles indicate in-frame mutations with deletions and insertions. Black spots indicate the late infantile type of NP-C, gray indicates the juvenile type, and white indicates the adult type. Underlines indicate new mutations reported in this paper. Fs, frameshift; and del, deletion.

Table 1
Clinical features of NP-C patients

| Clinical type | Cell strain | Ethnic group origin | Sex | Onset of neurological signs | Neurological signs | Hepatospleno megaly | Outcome | Amino-acid change | |
|---|---|---|---|---|---|---|---|---|---|
| Late infantile | OHS | JPN | M | 1.5 years | Epilepsy, psychomotor delay | HSM | 1.5 years (alive) | C956Y | 837Fs-838X |
| | KUR | JPN | F | 2.5 years | Epilepsy, deterioration | HSM | ? | R518Q | R518Q (homo) |
| | UET | JPN | F | 2 years | Deterioration, cataplexy, spastic tetraplegy | No | 4 years (alive) | R518Q | R518Q (homo) |
| | TAN | JPN | M | 2.5 years | Epilepsy, ataxia, deterioration | Mild SM | ? | R518Q | T1205R |
| | UCH | JPN | F | 2.5 years | Ataxia, deterioration | HSM | 5 years (dead) | H510P | H510P (homo) |
| | AMA | JPN | F | 3 years | Epilepsy, psychomotor delay | HSM | 4 years (alive) | C177G | 119Fs-130X |
| | YAM | JPN | M | 2 years 1 months | Ataxia, deterioration | HSM | 3 years 9 months (alive) | V1065G | 1206Fs-1241X |
| | GM110 | Caucasian | M | 5 years | Epilepsy, deterioration | ? | 10 years (alive) | I1061T | 740-741FS del (in frame deletion) |
| | NAK | JPN | M | 4 years 3 months | Epilepsy, deterioration | No | 4 years 3 months (alive) | G1236E | ? |
| Juvenile | SAS | JPN | F | 13 years | Epilepsy, ataxia, deterioration | Mild SM | 17 years (alive) | 16Fs-56X | ? |
| | END | JPN | M | 15 years | Dystonia, ataxia, VSO | Mild SM | 17 years (alive) | Y1088C | L1213F |
| | END2 | JPN | F | 14 years | Dystonia, ataxia, VSO | Mild SM | 15 years (alive) | Y1088C | L1213F |
| Adult type | KAI | JPN | M | 25 years | Dementia, ataxia, dystonia, epilepsy, VSO | SM | 42 years (dead) | V889M | 1015-1032GHAAYSSAVNILLGHGTRdel (in-frame) |

M, male; F, female; JPN, Japanese; HSM, hepatosplenomegaly; SM, splenomegaly; VSO, vertical supranuclear ophthalmoplegia; Fs, frame shift; X, stop; del, deletion; homo, homozygous; underlines, new mutations reported in this study.

All patients were unrelated, with the exception of END and END2, who were siblings. Primary cell cultures derived from patients' skin fibroblasts were collected after informed consent. Sixty-four normal control DNA samples were obtained from blood given by Japanese volunteers. Control skin fibroblast samples were also collected from volunteers.

### 2.2. Molecular analysis

DNA was extracted from cell cultures by proteinase K digestion followed by phenol-chloroform extraction [13]. Total RNA was isolated using the guanidinium thiocyanate extraction method [15]. The following procedures summarize the analysis of genomic mutations in skin fibroblast DNA of NP-C patients. All exons of *NPC1* were amplified by polymerase chain reaction (PCR) as described previously [14]. Mutation screening was carried out by single-strand conformational polymorphism (SSCP) analysis [14]. PCR products showing aberrant bands were directly sequenced using a BigDye terminator cycle sequencing kit (Applied Biosystems, USA) according to the manufacturer's recommendations. Both strands of each PCR product were sequenced with the same primers that were used for PCR. Sequence data were obtained using an ABI PRISM 3100 genetic analyzer (ABI) and results were analyzed with Genetyx computer

software (Software Development, Tokyo, Japan). A population study involving 64 normal control samples was performed to confirm the absence of frequent polymorphisms in the *NPC1* gene.

### 2.3. Northern blotting

Total RNA (20 μg) from each patient or control subject was subjected to electrophoresis on a 1% agarose/0.6 M formaldehyde gel, and subsequently transferred to a nylon membrane (Hybond-$N^+$, Amersham Pharmacia Biotech, Buckinghamshire, UK). After UV crosslinking (Funakoshi, Tokyo, Japan) and prehybridization at 68°C for 20 min with PerfectHyb (TOYOBO), the membrane was hybridized for 2 h with *NPC1* cDNA probe (kindly provided by Dr Peter G. Pentchev) labeled with [$\alpha$-$^{32}$P] dCTP (Amersham Pharmacia Biotech) by means of the BcaBest labeling kit (Takara, Tokyo, Japan). The membrane was washed twice with 2 × SSC (Sodium Chloride, Sodium Citrate) containing 0.1% SDS at 68°C for 5 min, and twice with 0.1 × SSC/0.1% SDS at 68°C for 15 min. Radioactive bands were visualized using the Bio-Rad Molecular Imager. The blots were also stripped and probed with human beta-actin cDNA as an internal control.

## 3. Results

### 3.1. NPC1 mutations

All mutations identified in this study are depicted in a schematic representation of the secondary structure of *NPC1* shown in Fig. 2. A novel one-base-pair deletion in exon 16 at nucleotide 2508 or 2509 (c.2508[-2509]A del) was identified in patient OHS (Table 1). This mutation resulted in a frameshift at amino acid 837 and created a stop codon at position 838 (837Fs-838X), predicating a truncated protein. Therefore, this mutation was considered to be a disease-causing mutation. A second novel mutation was identified in patient YAM. This missense mutation involved a T-to-G transversion at nucleotide 3194 in exon 21 (T3194G), resulting in the substitution of valine for glycine at position 1065 (V1065G) (Table 1). This mutation was considered to be a disease-causing mutation since it was not found in any of the normal controls. Patient YAM also carried a previously known mutation, c.3615[-3618]A del (1206Fs-1241X) [14], in exon 24.

In patient NAK, a 32-base pair deletion was identified in a non-coding intronic sequence, IVS13 -40-9 32-bp del. To ascertain whether this was a disease-causing mutation, we analyzed the cDNA sequence corresponding to exons 13–15 and found no aberrant splicing product (data not shown). Therefore, this deletion appeared to represent a normal variant.

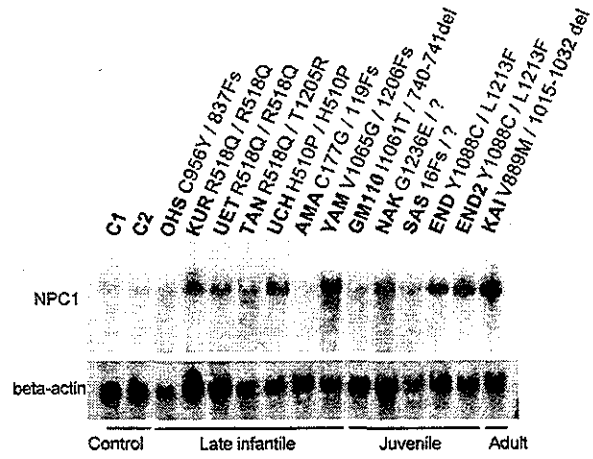


Fig. 3. Northern blot analysis of *NPC1* mRNA in cultured fibroblasts from NP-C patients. Total RNA (20 μg) in each lane was probed with $^{32}$P-labeled DNA fragments of *NPC1* cDNA (upper lane) and human beta-actin (bottom lane). RNA from 13 patients (Table 1) with late infantile, juvenile or adult onset NP-C was analyzed as indicated. C1 and C2 represent normal control RNA. Fs, frameshift; and del, deletion.

### 3.2. Northern blotting

To further understand NP-C pathophysiology, *NPC1* mRNA levels were examined in patient cultured skin fibroblasts (Fig. 3). We found that nine (KUR, UET, TAN, UCH, YAM, NAK, END, END2, and KAI) of the 13 samples exhibited increased levels of *NPC1* mRNA compared to normal controls. Of the seven patients in the late infantile type, five (KUR, UET, TAN, UCH, and YAM) showed increased mRNA levels. With the exception of YAM, all alleles of these five patients contained missense mutations. Two patients, KUR and UET, had the same genotype (homozygous for R518Q). The remaining two patients in this group, OHS and AMA, had a frameshift mutation in one allele and exhibited normal *NPC1* mRNA expression (Fig. 3). In the juvenile type, END and END2, siblings with the same genotype (Y1088C, L1213F), showed increased *NPC1* mRNA levels. NAK who had a missense mutation only in an allele showed increased level. SAS with a frameshift mutation and GM110 with an in-frame deletion showed almost same amount of mRNA with normal controls. In the adult type, KAI also showed an increased *NPC1* mRNA level.

## 4. Discussion

Since the discovery of the *NPC1* gene [9], we have identified a total of 31 different disease-causing mutations in Japanese NP-C patients [13,14]. Many other research groups have also identified *NPC1* mutations, and a total of 122 different *NPC1* mutations have been described including the two novel mutations reported in this study [13,14,16–24]. All of the known *NPC1* mutations are

depicted in Fig. 1, which clearly shows the clustering of mutations on the cysteine-rich loop previously described by Greer et al. [17].

In this study, two novel NP-C-related mutations were identified. One mutation is localized to the cysteine-rich luminal loop and the second is in the transmembrane region (Fig. 2). Almost all known *NPC1* mutations have been reported as single instances; however, a few occur frequently. I1061T is a common mutant allele in Western countries and correlates with a classic juvenile phenotype [18]. In this study, one patient showed the recurrent mutation, 1206Fs-1241X, in exon 24. In the 21 Japanese patients investigated in our laboratory, R518Q and 1206Fs-1241X were found in seven and four alleles, respectively, suggesting that these are relatively common mutations in Japanese patients [13,14].

It is difficult to make genotype-phenotype correlations because patients with mutations affecting the cysteine-rich loop show phenotypic variability. Therefore, additional information on *NPC1* mutations is required to further elucidate such relationships. An understanding of the molecular mechanisms underlying NP-C will enable practical prenatal diagnosis [25].

Previously, we quantified NPC1 levels in membrane preparations from cultured fibroblasts to investigate the impact of *NPC1* mutations on protein expression [14]. In the late infantile form (the most severe form of NP-C), there is a clear reduction in NPC1 levels and in some cases it is undetectable [14]. This evidence indicates that the amount of expressed protein correlates with a particular phenotype.

To date, there has been no published study focusing on the expression of *NPC1* mRNA but only just one about mouse mutant $npc^{nih}$ having a frameshift mutation, resulting in premature truncation of the open reading frame [25]. Loftus et al. demonstrated their data with a marked reduction of *Npc1* mRNA levels in the tissues derived from $npc^{nih}/npc^{nih}$ [26]. In our study, we showed the expressed amount of *NPC1* mRNA in the cells derived from human skin fibroblasts. Using Northern blots, we showed that patients carrying only missense mutations (KUR, UET, TAN, UCH, END, and KAI) showed increased levels of *NPC1* mRNA. However, some patients having at least one frameshift mutation (OHS, AMA, and SAS) displayed nearly normal levels of *NPC1* mRNA. One plausible explanation for this finding is that *NPC1* mRNA expression from the alleles of missense mutations is increased to compensate for loss of function. On the other hand, transcription of mRNA from alleles containing frameshift mutations appears to be inhibited or restrained same as $npc^{nih}/npc^{nih}$ mouse [26].

The only discrepancy between the present results and our previous Western blot results [14] is that the patients with missense mutations who presented with the late infantile form of NP-C have decreased levels of NPC1 despite having increased levels of *NPC1* mRNA. From this evidence we speculate that mutant NPC1 translated from mRNAs containing missense mutations may not exhibit proper tertiary structure and thus may exhibit reduced activity.

It remains unexplained as to why neuronal cells die in patients with NP-C. However, our present data may provide clues toward a resolution of this issue, and additional characterization of NP-C-associated mutations will further our knowledge of the genetic and molecular bases for this disease.

## Acknowledgements

This work was supported through a special grant from the Ministry of Health, Labour and Welfare of Japan, and by the Ministry of Education, Culture, Sports, Science and Technology of Japan with a grant in aid for scientific research.

## References

[1] Patterson MC, Vanier MT, Suzuki K, Morris JA, Carstea ED, Neufeld EB, et al. Niemann-Pick disease type C: a lipid trafficking disorder. In: Scriver CR, Beaudet AL, Sly WS, Valle D, Childs B, Kinzler KW, et al., editors. The metabolic and molecular bases of inherited disease, 8th ed. New York: McGraw-Hill; 2001. p. 3611–34.

[2] Vanier MT, Suzuki K. Niemann-Pick diseases. In: Moser HW, editor. Handbook of clinical neurology (neurodystrophies and neurolipidoses). Amsterdam: Elsevier; 1996. p. 133–62.

[3] Rodriguez-Lafrasse C, Rousson R, Pentchev PG, Louisot P, Vanier MT. Free sphingoid bases in tissues from patients with type C Niemann-Pick disease and other lysosomal storage disorders. Biochim Biophys Acta 1994;1226:138–44.

[4] Steinberg SJ, Ward CP, Fensom AH. Complementation studies in Niemann-Pick disease type C indicate the existence of a second group. J Med Genet 1994;31:317–20.

[5] Vanier MT, Duthel S, Rodriguez-Lafrasse C, Pentchev P, Carstea ED. Genetic heterogeneity in Niemann-Pick C disease: a study using somatic cell hybridization and linkage analysis. Am J Hum Genet 1996;58:118–25.

[6] Akaboshi S, Yano T, Miyawaki S, Ohno K, Takeshita K. A C57BL/KsJ mouse model of Niemann-Pick disease (spm) belongs to the same complementation group as the major childhood type of Niemann-Pick disease type C. Hum Genet 1997;99:350–3.

[7] Kurimasa A, Ohno K, Oshimura M. Restoration of the cholesterol metabolism in 3T3 cell lines derived from the sphingomyelinosis mouse (spm/spm) by transfer of a human chromosome 18. Hum Genet 1993;92:157–62.

[8] Carstea ED, Polymeropoulos MH, Parker CC, Detera-Wadleigh SD, O'Neill RR, Patterson MC, et al. Linkage of Niemann-Pick disease type C to human chromosome 18. Proc Natl Acad Sci USA 1993;90: 2002–4.

[9] Carstea ED, Morris JA, Coloman KG, Loftus SK, Zhang D, Cummings C, et al. Niemann-Pick C1 disease gene: homology to mediators of cholesterol homeostasis. Science 1997;277:228–31.

[10] Kobayashi T, Beuchat MH, Lindsay M, Frias S, Palmiter RD, Sakuraba H, et al. Late endosomal membranes rich in lysobisphosphatidic acid regulate cholesterol transport. Nat Cell Biol 1999;1: 113–8.

[11] Morris JA, Zhang D, Coleman KG, Nagle J, Pentchev PG, Carstea ED. The genomic organization and polymorphism analysis of

the human Niemann-Pick C1 gene. Biochem Biophys Res Commun 1999;261:493–8.

[12] Davies JP, Ioannou YA. Topological analysis of Niemann-Pick C1 protein reveals that the membrane orientation of the putative sterol-sensing domain is identical to those of 3-hydroxy-3-methylglutaryl-CoA reductase and sterol regulatory element binding protein cleavage-activating protein. J Biol Chem 2000;275:24367–74.

[13] Yamamoto T, Nanba E, Ninomiya H, Higaki K, Taniguchi M, Zhang H, et al. NPC1 gene mutations in Japanese patients with Niemann-Pick disease type C. Hum Genet 1999;105:10–16.

[14] Yamamoto T, Ninomiya H, Matsumoto M, Ohta Y, Nanba E, Tsutsumi Y, et al. Genotype-phenotype relationship of Niemann-Pick disease type C: a possible correlation between clinical onset and levels of NPC1 protein in isolated skin fibroblasts. J Med Genet 2000;37: 707–11.

[15] Sambrook J, Russell DW. Purification of RNA from cells and tissues by acid phenol-guanidinium thiocyanate-chloroform extraction. In: Sambrook J, Russell DW, editors. Molecular cloning: a laboratory manual, 3rd ed. New York: Cold Spring Harbor Laboratory Press; 2001. p. 7.4–7.7.

[16] Greer WL, Riddell DC, Gillan TL, Girouard GS, Sparrow SM, Byers DM, et al. The Nova Scotia (type D) form of Niemann-Pick disease is caused by a G3097 → T transversion in NPC1. Am J Hum Genet 1998;63:52–4.

[17] Greer WL, Dobson MJ, Girouard GS, Byers DM, Riddell DC, Neumann PE. Mutations in NPC1 highlight a conserved NPC1-specific cysteine-rich domain. Am J Hum Genet 1999;65: 1252–60.

[18] Millat G, Marcais C, Rafi MA, Yamamoto T, Morris JA, Pentchev PG, et al. Niemann-Pick C1 disease: the I1061T substitution is a frequent mutant allele in patients of Western European descent and correlates with a classic juvenile phenotype. Am J Hum Genet 1999;65:1321–9.

[19] Millat G, Marcais C, Tomasetto C, Chikh K, Fensom AH, Harzer K, et al. Niemann-Pick C1 disease: correlations between NPC1 mutations, levels of NPC1 protein, and phenotypes emphasize the functional significance of the putative sterol-sensing domain and of the cysteine-rich luminal loop. Am J Hum Genet 2001;68:1373–85.

[20] Ribeiro I, Marcao A, Amaral O, Sa Miranda MC, Vanier MT, Millat G. Niemann-Pick type C disease: NPC1 mutations associated with severe and mild cellular cholesterol trafficking alterations. Hum Genet 2001;109:24–32.

[21] Sun X, Marks DL, Park WD, Wheatley CL, Puri V, O'Brien JF, et al. Niemann-Pick C variant detection by altered sphingolipid trafficking and correlation with mutations within a specific domain of NPC1. Am J Hum Genet 2001;68:1361–72.

[22] Meiner V, Shpitzen S, Mandel H, Klar A, Ben-Neriah Z, Zlotogora J, et al. Clinical-biochemical correlation in molecularly characterized patients with Niemann-Pick type C. Genet Med 2001;3:343–8.

[23] Bauer P, Knoblich R, Bauer C, Finckh U, Hufen A, Kropp J, et al. NPC1: Complete genomic sequence, mutation analysis, and characterization of haplotypes. Hum Mutat 2002;19:30–8.

[24] Saito Y, Suzuki K, Nanba E, Yamamoto T, Ohno K, Murayama S. Niemann-Pick type C disease: accelerated neurofibrillary tangle formation and amyloid β deposition associated with APOE ϵ4 homozygosity. Ann Neurol 2002;52:351–5.

[25] Tsukamoto H, Yamamoto T, Nishigaki T, Sakai N, Nanba E, Ninomiya H, et al. SSCP analysis by RT-PCR for the prenatal diagnosis of Niemann-Pick disease type C. Prenat Diagn 2001;21: 55–7.

[26] Loftus SK, Morris JA, Carstea ED, Gu JZ, Cummings C, Brown A, et al. Murine model of Niemann-Pick C disease: mutation in a cholesterol homeostasis gene. Science 1997;277:232–5.

Available online at www.sciencedirect.com

SCIENCE DIRECT®

Biochimica et Biophysica Acta 1689 (2004) 219–228

BIOCHIMICA ET BIOPHYSICA ACTA
BBA

www.bba-direct.com

# *N*-Octyl-β-valienamine up-regulates activity of F213I mutant β-glucosidase in cultured cells: a potential chemical chaperone therapy for Gaucher disease

Hou Lin[a,1], Yuko Sugimoto[b], Yuki Ohsaki[b], Haruaki Ninomiya[b], Akira Oka[a], Miyako Taniguchi[b], Hiroyuki Ida[c], Yoshikatsu Eto[c], Seiichiro Ogawa[d], Yuji Matsuzaki[e], Miwa Sawa[e], Takehiko Inoue[a], Katsumi Higaki[f], Eiji Nanba[f], Kousaku Ohno[a,*], Yoshiyuki Suzuki[g]

[a] *Department of Neurobiology, Division of Child Neurology, Tottori University Faculty of Medicine, 86 Nishi-machi, Yonago 683-8504, Japan*
[b] *Department of Neurobiology, Tottori University Faculty of Medicine, Yonago 683-8503, Japan*
[c] *Departments of Pediatrics and Gene Therapy, Institute of DNA Medicine, Jikei University, Tokyo 105-8461, Japan*
[d] *Department of Applied Chemistry, Faculty of Science and Technology, Keio University, Yokohama 223-8522, Japan*
[e] *Central Research Laboratories, Seikagaku Corporation, Tokyo 207-0021, Japan*
[f] *Gene Research Center, Tottori University, Yonago, 683-8503, Japan*
[g] *Clinical Research Center, International University of Health and Welfare, Otawara 324-8501, Japan*

Received 3 October 2003; received in revised form 22 March 2004; accepted 25 March 2004
Available online 22 April 2004

Available online at www.sciencedirect.com
SCIENCE DIRECT®
Biochimica et Biophysica Acta 1689 (2004) 219–228
BIOCHIMICA ET BIOPHYSICA ACTA
BBA
www.bba-direct.com

# *N*-Octyl-β-valienamine up-regulates activity of F213I mutant β-glucosidase in cultured cells: a potential chemical chaperone therapy for Gaucher disease

Hou Lin[a,1], Yuko Sugimoto[b], Yuki Ohsaki[b], Haruaki Ninomiya[b], Akira Oka[a], Miyako Taniguchi[b], Hiroyuki Ida[c], Yoshikatsu Eto[c], Seiichiro Ogawa[d], Yuji Matsuzaki[e], Miwa Sawa[e], Takehiko Inoue[a], Katsumi Higaki[f], Eiji Nanba[f], Kousaku Ohno[a,*], Yoshiyuki Suzuki[g]

[a] *Department of Neurobiology, Division of Child Neurology, Tottori University Faculty of Medicine, 86 Nishi-machi, Yonago 683-8504, Japan*
[b] *Department of Neurobiology, Tottori University Faculty of Medicine, Yonago 683-8503, Japan*
[c] *Departments of Pediatrics and Gene Therapy, Institute of DNA Medicine, Jikei University, Tokyo 105-8461, Japan*
[d] *Department of Applied Chemistry, Faculty of Science and Technology, Keio University, Yokohama 223-8522, Japan*
[e] *Central Research Laboratories, Seikagaku Corporation, Tokyo 207-0021, Japan*
[f] *Gene Research Center, Tottori University, Yonago, 683-8503, Japan*
[g] *Clinical Research Center, International University of Health and Welfare, Otawara 324-8501, Japan*

Received 3 October 2003; received in revised form 22 March 2004; accepted 25 March 2004
Available online 22 April 2004

**Abstract**

Gaucher disease (GD) is the most common form of sphingolipidosis and is caused by a defect of β-glucosidase (β-Glu). A carbohydrate mimic *N*-octyl-β-valienamine (NOV) is an inhibitor of β-Glu. When applied to cultured GD fibroblasts with F213I β-Glu mutation, NOV increased the protein level of the mutant enzyme and up-regulated cellular enzyme activity. The maximum effect of NOV was observed in F213I homozygous cells in which NOV treatment at 30 μM for 4 days caused a ~ 6-fold increase in the enzyme activity, up to ~ 80% of the activity in control cells. NOV was not effective in cells with other β-Glu mutations, N370S, L444P, 84CG and RecNciI. Immunofluorescence and cell fractionation showed localization of the F213I mutant enzyme in the lysosomes of NOV-treated cells. Consistent with this, NOV restored clearance of $^{14}$C-labeled glucosylceramide in F213I homozygous cells. F213I mutant β-Glu rapidly lost its activity at neutral pH in vitro and this pH-dependent loss of activity was attenuated by NOV. These results suggest that NOV works as a chemical chaperone to accelerate transport and maturation of F213I mutant β-Glu and may suggest a therapeutic value of this compound for GD.


*Keywords:* Gaucher disease; β-glucosidase; Valienamine; Glucosylceramide; Chaperone

## 1. Introduction

Gaucher disease (GD) is an inherited lipid storage disorder, characterized by lysosomal accumulation of glucocerebroside (glucosylceramide; GlcCer) in monocyte-macrophage cells [1]. It is caused by a defect of acid β-glucosidase (β-Glu; glucocerebrosidase EC 3.2.1.45). Patients with GD exhibit hepatosplenomegaly, anemia, bone lesions and respiratory failure, with or without progressive neurological symptoms. Patients without neurological symptoms are classified as type 1, whereas those with neurological symptoms are classified into type 2 (acute infantile form) and type 3 (juvenile form).

*Abbreviations:* α-Gal A, α-galactosidase A; α-Glu, α-glucosidase; β-Gal, β-galactosidase; β-Glu, β-glucosidase; β-Hex, β-hexosaminidase; NOEV, *N*-octyl-β-epi-valienamine; NOV, *N*-octyl-β-valienamine; DGJ, 1-deoxy-galactonojirimycin; ER, endoplasmic reticulum; GD, Gaucher disease; GlcCer, glucosylceramide; HPTLC, high performance thin layer chromatography; NN-DGJ, *N*-(*n*-nonyl)-deoxy-nojirimaycin

* Corresponding author. Tel.: +81-859-34-8037; fax: +81-859-34-8135.
*E-mail address:* ohno@grape.med.tottori-u.ac.jp (K. Ohno).
[1] Present address: Department of Biochemistry, Medical College, Qingdao University, Qingdao, Shandong 266021, PR China.

0925-4439/$ - see front matter © 2004 Elsevier B.V. All rights reserved.
doi:10.1016/j.bbadis.2004.03.007

Current therapeutic strategies for GD include enzyme replacement and substrate depletion. Enzyme replacement has been achieved by intravenous administration of macrophage-targeted recombinant β-Glu [2] and it has been proven to be quite effective for visceral, hematologic and skeletal abnormalities [3,4]. Unfortunately, the efficacy to neurological manifestations of this therapy is, if any, limited [5–7]. A high cost as well as necessity to continue the infusion every 2 weeks is not negligible, when indication of enzyme replacement is considered in practice [4]. Substrate depletion has been achieved by oral administration of *N*-butyl-deoxynojirimycin, which inhibits glucosyltransferase and decreases substrate biosynthesis. This therapy has been reported to be beneficial for non-neuropathic GD [8,9].

We have proposed a novel therapeutic strategy for glycolipid storage disorders to accelerate transport and maturation of mutant enzymes by using enzyme inhibitors as a chemical chaperone. This strategy was first applied to Fabry disease (α-galactosidase A [α-Gal A] deficiency) and we found that 1-deoxy-galactonojirimycin (DGJ), an inhibitor of α-Gal A, markedly enhanced activity of mutant enzymes in lymphoblasts from Fabry patients [10]. Although up-regulation of enzyme activity by an inhibitor appeared paradoxical, evidence was presented that DGJ prevented pH-dependent degradation of mutant α-Gal A at the site of its synthesis [i.e., the endoplasmic reticulum (ER)]. With the aid of DGJ, mutant α-Gal A escaped the ER quality control system and was transported to the lysosome where it is stabilized because of the acidic condition and restored cellular enzyme activity. This strategy was then tested in GM1-galactosidosis [β-galactosidase (β-Gal) deficiency] and we found that DGJ as well as another derivative *N*-(*n*-butyl)-deoxy-galactonojirimycin could up-regulate activity of mutant human β-Gal expressed in fibroblasts from β-Gal knockout mice [11]. In pursuit of the same therapeutic strategy, Sawkar et al. [12] reported that an inhibitor of β-Glu, *N*-(*n*-nonyl)-deoxynojirimaycin (NN-DNJ) up-regulated activity of N370S mutant β-Glu in GD fibroblasts. Although it is yet to be tested whether NN-DNJ can correct GlcCer accumulation in N370S GD cells, their findings suggested that this strategy might be extended to GD.

Valienamine is a synthetic carbohydrate mimic and we have prepared various *N*-alkyl and *N*,*N*-dialkyl-β-valienamines in continuation of a chemical modification program [13]. Among these substances, *N*-octyl-β-epivalienamine (NOEV) is an inhibitor of β-Gal and we have provided evidence that NOEV worked as a chemical chaperone to up-regulate mutant β-Gal activity both in cultured cells and in mice [14]. *N*-octyl-β-valienamine (NOV) is an isomer of NOEV and exerted the strongest inhibition of β-Glu activity in the mouse liver [15]. The purpose of the current studies was to test a possibility that NOV could up-regulate mutant β-Glu activity in cultured human cells. Preliminary findings of the current studies have been reported [16].

## 2. Materials and methods

### 2.1. Materials

Dulbecco's Modified Eagle's Medium (DMEM), fetal calf serum (FCS) and dialyzed serum were obtained from GibcoBRL. NOV was synthesized in our laboratory (Central Research Laboratories, Seikagaku). Stock solution of NOV was prepared in $H_2O$ at 3 mM and stored at −20 °C. A mouse monoclonal antibody against human β-Glu (clone 8E4, Ref. [17]) was a kind gift from Dr. Barranger JA. Rabbit polyclonal anti-hexosaminidase A (HexA) has been described [18]. Rabbit polyclonal anti-calnexin was from Calbiochem. [1-$^{14}$C]Serine (1.85 GBq/mmol) was from American Radiolabeled Chemicals (St. Louis, MO).

### 2.2. Cell culture

Human skin fibroblasts were cultured in DMEM/10% FCS at 37 °C in 5% $CO_2$. We used two lines of control cells (H11, H34) and five lines of GD cells with β-Glu mutations of 754A(F213I)/754A(F213I), 754A(F213I)/1448C(L444P), 1126G(N370S)/84GG, 1448C(L444P)/RecNciI, and 1448C(L444P)/1448C(L444P) [19]. 84GG causes premature termination of the encoded protein and RecNciI causes amino acid substitutions L444P and A456P [1]. Culture medium was replaced every 2 days with fresh media supplemented with or without NOV at the concentrations indicated.

### 2.3. Enzyme assays

Lysosomal enzyme activities in cell lysates were determined as described [14,18,20,21]. Briefly, cells were scraped into ice-cold $H_2O$ ($10^6$/ml) and lysed by sonication. Insoluble materials were removed by centrifugation at 12,000 × *g* for 10 min at 4 °C and protein concentrations were determined with a BCA microprotein assay kit (Piearce). Ten microliters of the lysates was incubated at 37 °C with 20 μl of the substrate solution in 0.1 M citrate buffer, pH 4.5. The substrates were 4-methylumbelliferone-conjugated β-D-galactopyranoside (for β-Gal, Ref. [14]), β-D-glucopyranoside (for β-Glu, Ref. [20]), α-D-glucoside (for α-Glu, Ref. [21]) and *N*-acetyl-β-D-glucosaminide (for β-Hex, Ref. [18]). The reaction was terminated by adding 1.0 ml of 0.2 M glycine sodium hydroxide buffer (pH 10.7). One unit of enzyme activity was defined as nanomoles of 4-methyl-umbelliferone released per hour.

### 2.4. Western blotting

Cell lysates (20 μg protein) were electrophoresed on a 10% SDS-PAGE and transferred to a PVDF membrane.

The blots were probed with antibodies against β-Glu (1:500) or HexA (1:1000) and developed with an ECL kit (Amersham Pharmacia). Densitometry was performed by using an NIH image software.

### 2.5. Immunofluorescence

We used staining procedures described previously [22]. Briefly, cells grown on cover glasses were fixed with 4% paraformaldehyde and permiabilized with 1% Triton X-100. Cells were incubated with anti-β-Glu (1:100), followed by Alexa488-conjugated anti-mouse IgG. Fluorescent images were collected by using a Bio-Rad MRC1024 confocal laser microscope. For localization of lysosomes, cells were exposed to Lysotracker Red (5 μg/ml; Molecular Probe) for 1 h prior to fixation.

### 2.6. Subcellular fractionation

Cell homogenates were fractionated by using Opti-prep (Axis-Shield plc., Dundee, UK) as described [23]. Briefly, cells were homogenized with a potter homogenizer in ice-cold buffer [HEPES 10 mM pH 7.0, 1 mM EDTA, 1 mM EGTA supplemented with a protease inhibitor cocktail (Boehringer)]. Homogenates were overlaid on Opti-prep and centrifuged at 100,000 × *g* for 16 h at 4 °C. Twelve fractions were recovered from the top and numbered accordingly.

### 2.7. Metabolic labeling of GlcCer

Cellular glycolipids were labeled with [$^{14}$C]serine as described [24]. Briefly, cells were cultured for 1 week in dialyzed serum supplemented with essential amino acids except for serine, and incubated with [$^{14}$C]serine (1 μCi/ml) for 3 days. The labeled cells were cultured in fresh DMEM/10% FCS for 5 days with or without NOV. We analyzed labeled lipids by high-performance thin layer chromatography (HPTLC) as described [25]. In brief, cells were harvested at the time indicated, and lipids were extracted with chloroform/methanol (2:1 v/v) and purified by an alkaline treatment. Neutral glycolipids were purified by C18 affinity chromatography. HPTLC was performed with chloroform/methanol/water (55:25:4) as a developing solvent. Labeled lipids were visualized by autoradiography (Fuji-BAS 2500: Fuji, Tokyo, Japan) and densitometry was performed using an NIH image software.

### 2.8. pH-dependent stability of β-Glu in vitro

Cell lysates were incubated in 0.1 M citrate-phosphate buffer at pH 5, 6 or 7 at 37 °C for the time indicated. Incubation was terminated by the addition of 3 volumes of 0.2 M citrate-phosphate buffer (pH 4.5), immediately followed by chilling on ice. The enzyme assay was done at pH 4.5 as described above.

## 3. Results

### 3.1. Inhibition of human β-Glu by NOV in vitro

Chemical structures of NOV and its isomer NOEV are shown in Fig. 1a. NOV inhibited β-Glu activity in mouse liver extracts with an $IC_{50}$ value of 0.03 μM [15]. To test whether it also works on the human enzyme, we determined β-Glu activity in lysates from control human fibroblasts in the absence or presence of NOV. NOV caused dose-dependent inhibition of β-Glu activity with an $IC_{50}$ value of 3 μM (Fig. 1b), indicating that it also works on human β-Glu. NOV contains a C8 fatty acid acyl moiety chain (Fig. 1a). A related compound with a C6

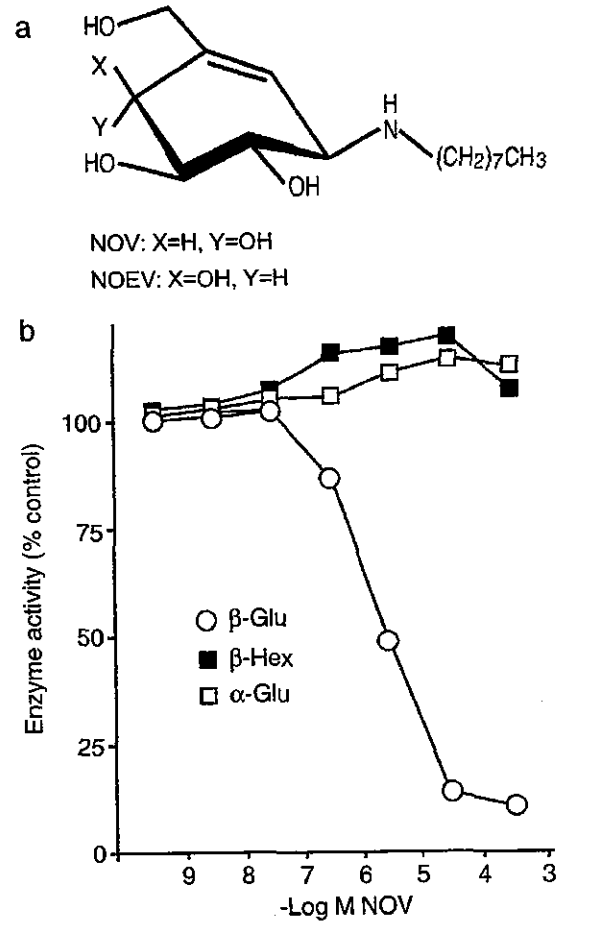


Fig. 1. Effects of NOV on lysosomal enzyme activities in lysates from control human fibroblasts. (a) Chemical structures of NOV and its isomer NOEV. (b) Dose dependence. Enzyme activity in H11 cell lysates was determined in the absence or presence of increasing concentrations of NOV. Each point represents means of triplicate determinations obtained in a single experiment. Values were expressed as relative to activity in the absence of NOV (100%). Values in the absence of NOV in this experiment were β-Glu 142, α-Glu 94 and β-Hex 5089 (units/mg protein). Similar results were obtained in two other experiments.

fatty acid acyl moiety chain inhibited human β-Glu with an $IC_{50}$ value of 30 μM (data not shown), suggesting that the inhibitory activity can be regulated by the length of this chain. NOV caused no inhibition of other lysosomal enzymes α-Glu and β-Hex in the same cell lysates, suggesting a specificity of NOV as an inhibitor of β-Glu (Fig. 1b).

### *3.2. Up-regulation of F213I mutant β-Glu activity in GD cells treated with NOV*

To explore an effect of NOV on mutant β-Glu activity, GD cells with five different genotypes were cultured for 4 days with increasing concentrations of NOV, and β-Glu activity in cell lysates was determined (Fig. 2a, right). NOV

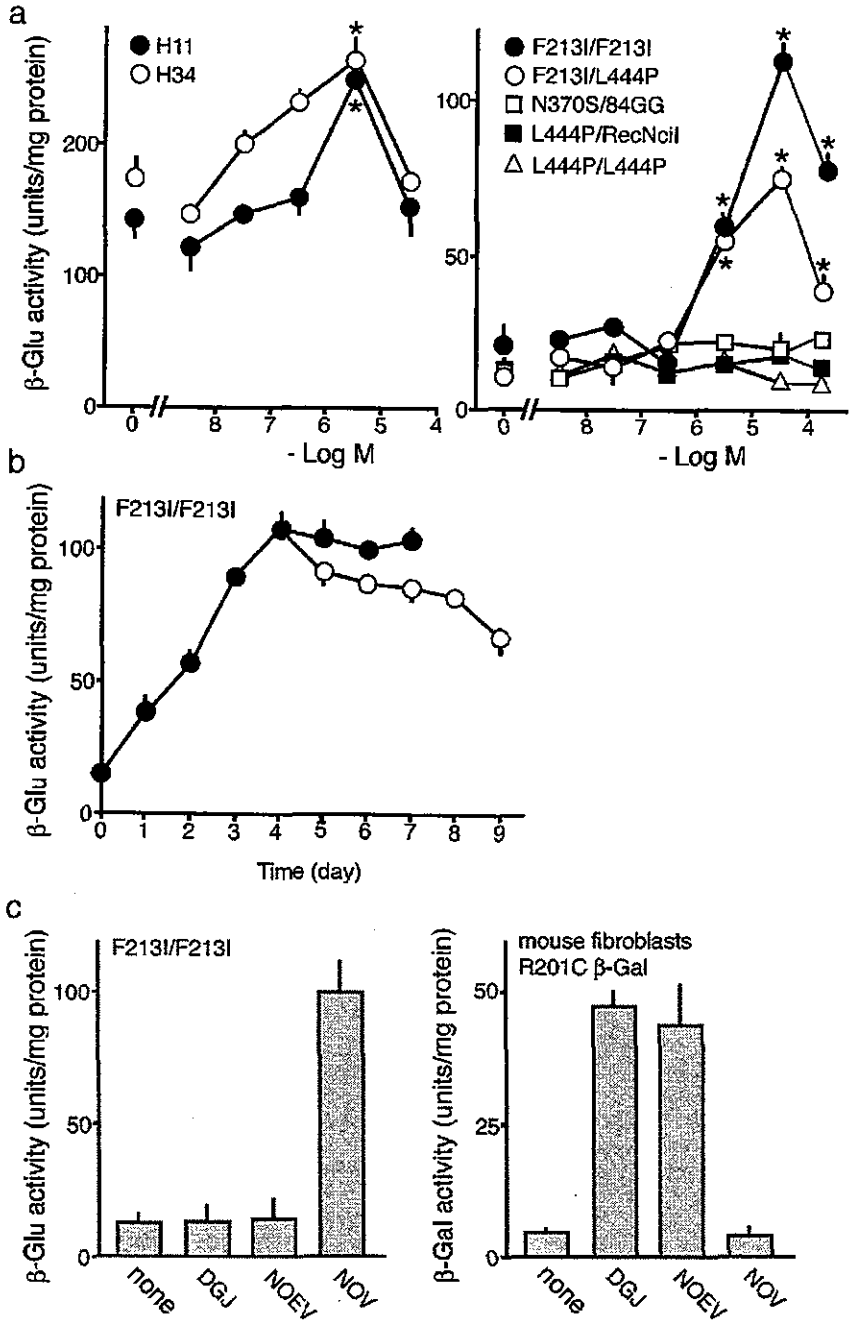


Fig. 2. Effects of NOV on cellular β-Glu activity. (a) Dose dependence. Two lines of control cells (left) and five lines of GD cells (right) were cultured for 4 days in the absence or presence of increasing concentrations of NOV and β-Glu activity in cell lysates was determined. (b) Time course. F213I/F213I cells were cultured in the presence of 30 μM NOV up to 7 days (●). A subset of cells was cultured with NOV for 4 days, washed and further cultured without the drug for 5 days (○). At the time indicated, cells were harvested and β-Glu activity in cell lysates was determined. (c) Specificity of the effects of NOV. F213I/F213I cells were cultured in the presence of indicated drugs (all at 20 μM) for 4 days and β-Glu activity in cell lysates was determined (left). In separate experiments, the same drugs were applied to mouse fibroblasts that express human R201C β-Gal and β-Gal activity in cell lysates was determined (right). Each point or bar represents mean ± S.E. of three determinations each done in triplicate. $*P<0.05$, statistically different from the values in the absence of the drug (*t* test).

caused dose-dependent increases in β-Glu activity in two lines of GD cells, F213I/F213I and F213I/L444P. The maximum effect of NOV was observed in F213I homozygous cells in which treatment at 30 μM caused a ~ 6-fold increase in the enzyme activity, up to ~ 80% of the basal activity in control cells. NOV at the same concentration caused a ~ 3-fold increase in F213I/L444P cells. There appeared to be an optimal concentration of NOV, because it was less potent at a higher concentration (100 μM). NOV caused no substantial increase in the enzyme activity of GD cells with other mutations, indicating a specificity of this up-regulation for F213I mutant β-Glu. This effect of NOV, however, was also observed in wild-type β-Glu with a different dose dependence profile; NOV at 3 μM caused a ~ 1.5-fold increase in the two control cell lines but was not effective at 30 μM (Fig. 2a, left).

Time-course analysis using F213I/F213I cells showed that in the presence of NOV (30 μM), β-Glu activity increased in a time-dependent manner and reached a plateau on day 4. When cells were deprived of NOV on

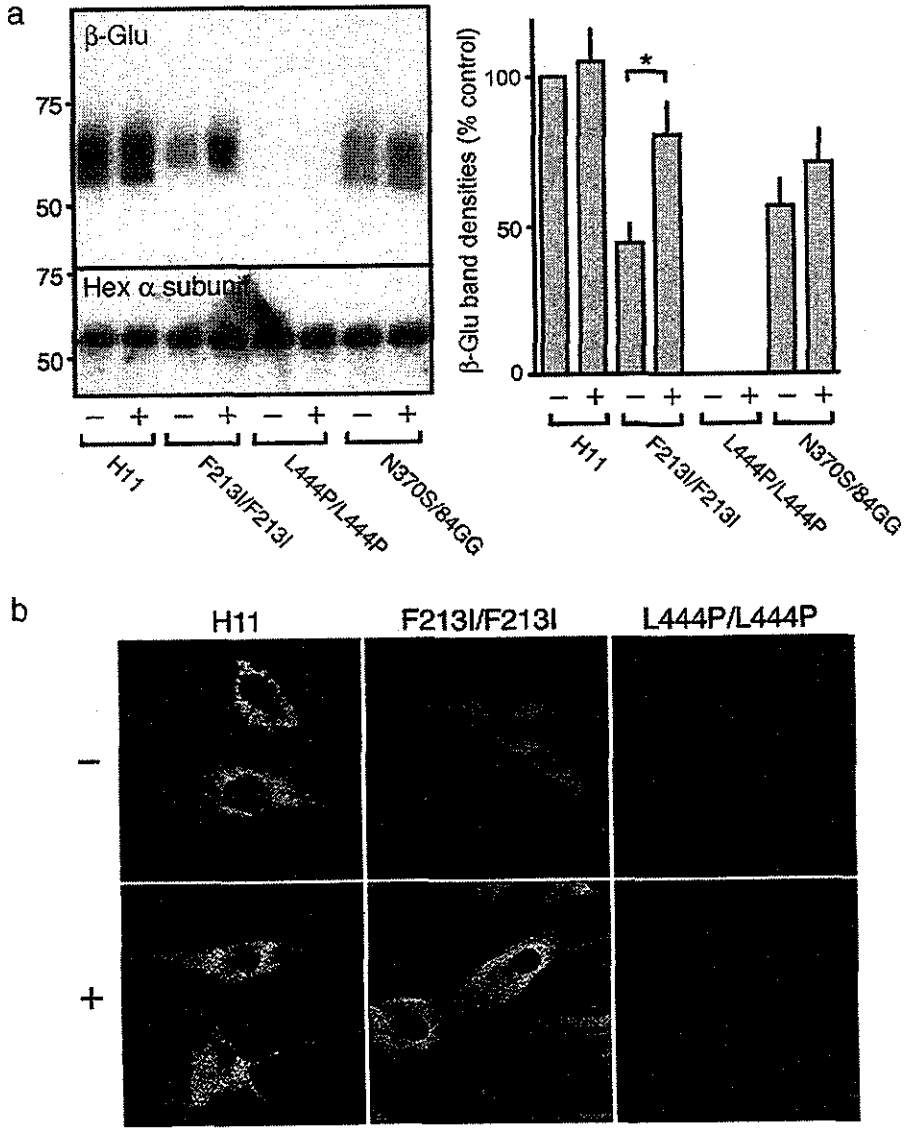


Fig. 3. Effects of NOV on the protein level and intracellular localization of mutant β-Glu. Cells were cultured with (+) or without (−) NOV at 30 μM for 4 days. (a) Western blotting. Cell lysates were analyzed by Western blotting with antibodies against β-Glu or Hex α subunit (left). Twenty micrograms of protein was loaded in each lane. Molecular weights are given on the left (kDa). Densities of β-Glu bands were quantified by densitometry (right). Each bar represents mean ± S.E. of 3 determinations. *$P<0.05$, statistically different from each other ($t$ test). (b) Anti-β-Glu immunofluorescence. (c) Double labeling of F213I/F213I cells with anti-β-Glu and Lysotracker Red. In b and c, shown are the representative images obtained with a confocal microscope. All the images were obtained at the same laser intensity and window level. (d) Cell fractionation. Cells were cultured with (●) or without (○) NOV at 30 μM for 4 days. Cell homogenates were subjected to Opti-prep fractionation and each fraction was assessed for activity of β-Glu (upper) or β-Hex (lower). Fractions from F213I/F213I cells were also subjected to anti-calnexin Western blotting. Each point represents mean values of triplicate determinations obtained in a single experiment. Similar results were obtained in two other experiments.

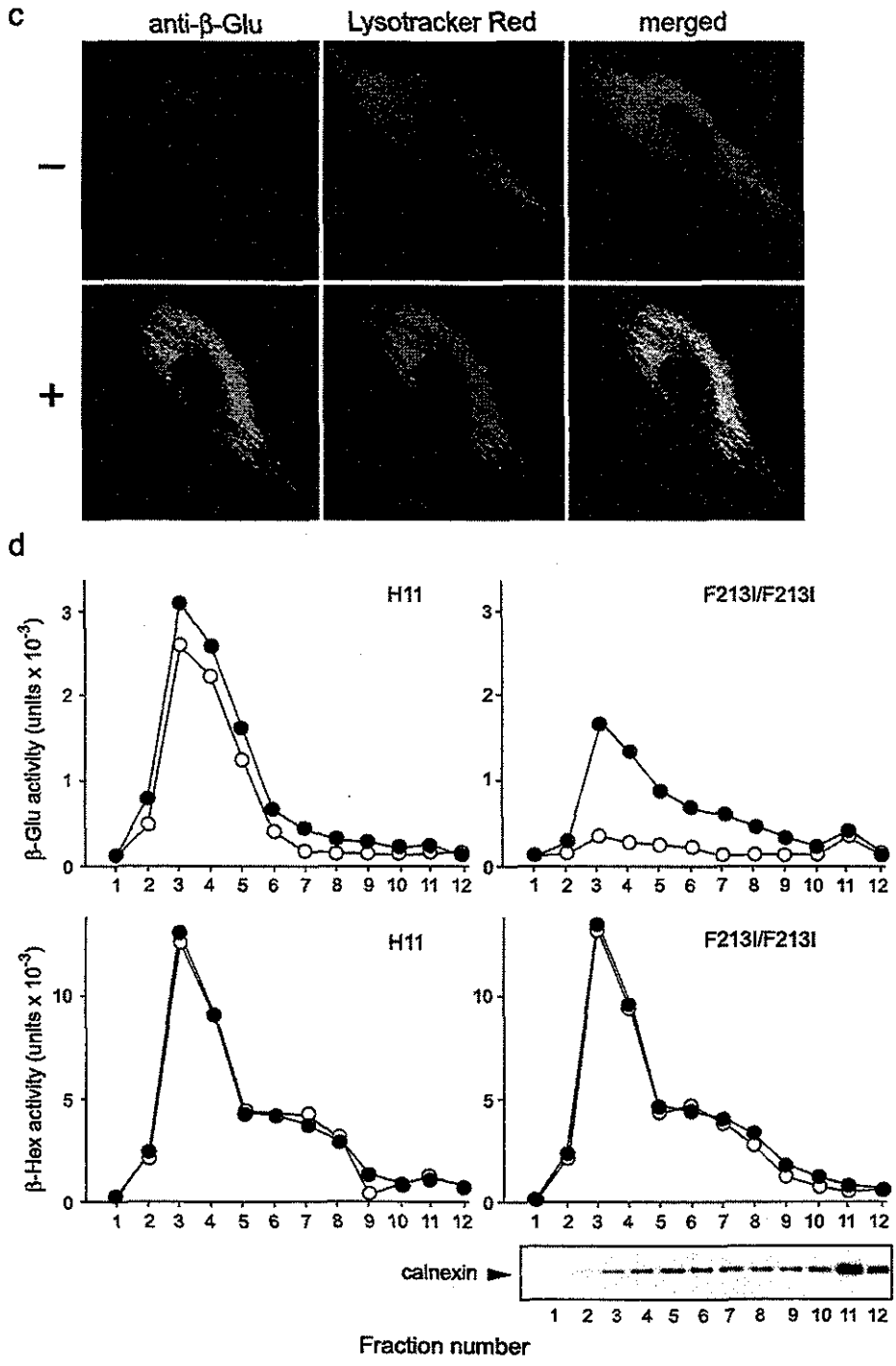


Fig. 3 (*continued*).

day 4, the activity gradually decreased thereafter but was still more than three times higher than the basal level on day 9 (Fig. 2b).

We have shown that both DGJ and NOEV could up-regulate the activity of R201C mutant β-Gal that was expressed in fibroblasts derived from β-Gal knockout mice [11,14]. To test specificity of NOV, first, we examined whether DGJ or NOEV could up-regulate F213I β-Glu activity, and found that neither of these substances caused any changes in the activity (Fig. 2c, left). Second, we examined whether NOV could up-regulate the activity of R201C mutant β-Gal, and found that unlike DGJ and NOEV, NOV had no effect on this mutant enzyme (Fig. 2c, right).

### 3.3. NOV increased the protein level of F213I mutant β-Glu and restored its localization in the lysosome

To examine the effect of NOV on the protein level, cell lysates were subjected to Western blotting with 8E4 monoclonal anti-β-Glu antibody and the protein levels were estimated by densitometry. This analysis showed that NOV treatment (30 μM for 4 days) of F213I/F213I cells caused a significant increase in the protein level of F213I mutant β-Glu. The same treatment did not increase the protein levels in N370S/84GG and control cells. As reported previously [26], the antibody did not recognize L444P mutant β-Glu. As a control, NOV treatment caused no changes in the protein levels of Hex α subunit (Fig. 3a).

Next, we examined intracellular localization of β-Glu by immunofluorescence and cell fractionation. Anti-β-Glu staining of control cells showed localization of β-Glu immunoreactivity in perinuclear punctate structures and this localization was not affected by NOV treatment. β-Glu immunoreactivity in F213I/F213I cells was lower than in control cells and there was no clear localization in perinuclear punctate structures. When these cells were treated with NOV, however, the immunoreactivity was clearly seen in these structures (Fig. 3b). Localization of F213I mutant β-Glu in the lysosome of NOV-treated cells was evidenced by co-localization of the immunoreactivity and a lysosome marker Lysotracker Red (Fig. 3c). β-Glu immunoreactivity was not detectable in L444P/L444P cells, indicating the specificity of this antibody staining (Fig. 3b).

When control cells were subjected to subcellular fractionation on Opti-prep, β-Glu activity was recovered in fractions #3–5. The same analysis of F213I/F213I cell fractions showed broad distribution of mutant β-Glu activity with peaks at #3 and #11. Both peaks were small but were consistently observed in three independent determinations. Anti-calnexin Western blotting showed that #11 contained a high amount of this ER marker protein [27]. NOV treatment of control cells caused marginal increases ( ~ 1.1-fold) in β-Glu activity recovered in #3–5. The same treatment of F213I/F213I cells caused ~ 4-fold increases in #3–5. As a control, we measured β-Hex activity in each fraction. Both in control and F213I/F213I cells, β-Hex activity was recovered in #3–4 and to a lesser degree, in #5–8. β-Hex activity in each fraction was not affected by NOV treatment in either cell line (Fig. 3d).

### 3.4. NOV restored clearance of $^{14}$C-labeled GlcCer in F213I/F213I cells

NOV-induced increase of mutant β-Glu activity in the lysosome of F213I/F213I cells prompted us to examine whether NOV could correct abnormal catabolism of GlcCer in this cell line. By using conventional HPTLC analysis of cellular lipid extracts, accumulation of GlcCer was barely detectable in GD skin fibroblasts, most likely because of the low level of this lipid in these cells (data not shown). Therefore, we employed metabolic labeling of cellular glycolipids with [$^{14}$C]serine and assessed clearance of $^{14}$C-labeled GlcCer. When control cells were chased for 5 days after the metabolic labeling, the content of $^{14}$C-GlcCer decreased by ~ 50%. This clearance of $^{14}$C-GlcCer was retarded in F213I/F213I cells in which there was only a ~ 10% decrease. Inclusion of NOV (30 μM) in the chase medium had no effect in control cells but accelerated the clearance in F213I/F213I cells. In the presence of NOV, the content of $^{14}$C-GlcCer in F213I/F213I cells decreased by ~ 50% and reached a level that was comparable to that in control cells (Fig. 4b). The HPTLC analyses showed that besides $^{14}$C-GlcCer, clearance of $^{14}$C-LacCer was retarded in F213I/F213I cell and again it was accelerated by NOV (Fig. 4a). In addition, NOV caused decreases in the levels of $^{14}$C-labeled lipids that corresponded to the positions of CTH, SM and

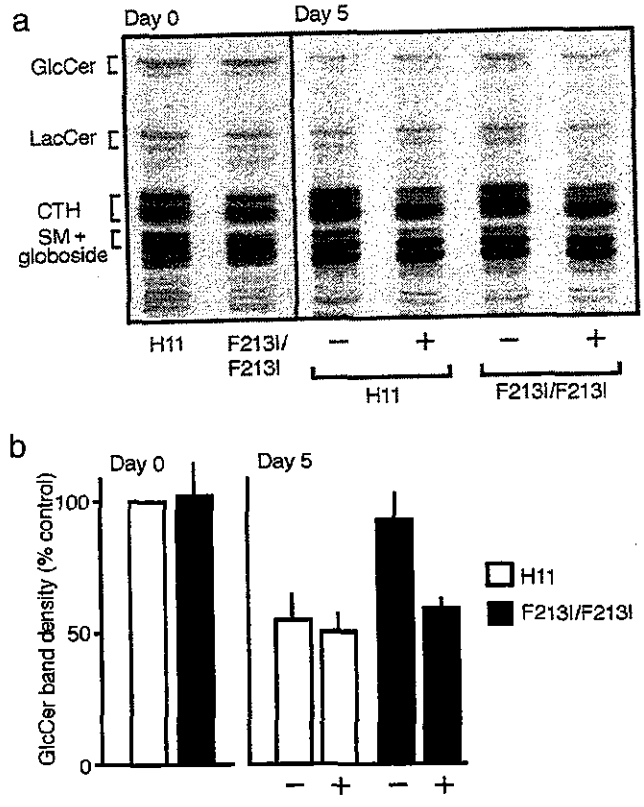


Fig. 4. Effects of NOV on cellular clearance of $^{14}$C-labeled GlcCer. (a) HPTLC separation of $^{14}$C-labeled cellular lipids. Cells were labeled with $^{14}$C-serine for 3 days and then chased up to 5 days in the presence or absence of NOV (30 μM). At the beginning (day 0) and the end (day 5) of the chase period, cells were harvested and neutral glycolipid fraction was analyzed by HPTLC. Positions of standard lipids are given on the left (LacCer, lactosylceramide; CTH, ceramide trihexoside; SM, sphingomyelin). (b) Densitometry. Densities of $^{14}$C-GlcCer bands on autoradiographs were quantified using an NIH image software. Values were expressed as relative to the band density of H11 cell extracts at the beginning of the chase period (day 0) as 100%. Each bar represents mean ± S.E. of three determinations.

globoside. The decreases, however, were observed both in control and F213I/F213I cells and the identities of these lipids were left unresolved.

### 3.5. NOV attenuated pH-dependent loss of F213I mutant β-Glu activity in vitro

Some mutations of lysosomal enzymes affect pH-dependent protein stability [1] and we reported that an α-Gal A inhibitor DGJ prevented in vitro degradation of mutant α-Gal A at neutral pH [10]. To examine whether a similar mechanism underlined NOV effects on F213I mutant β-Glu, we compared pH-dependent stability of wild-type and F213I mutant β-Glu and tested an effect of NOV. In these experiments, we used cell lysates prepared from untreated control cells and from F213I/F213I cells that had been treated with NOV at 30 μM for 4 days and further cultured without the drug for 1 day. When F213I/F213I cell lysates were incubated at pH 7, mutant β-Glu activity was rapidly lost and there remained less than 5% activity at 1 h. Mutant β-Glu activity also decreased in acidic conditions at pH 5 or 6, but ~ 60% activity retained at 1 h under these conditions. In contrast, there were only marginal decreases of wild-type β-Glu activity in control cell lysates and more than 80% activity retained after 1-h incubation at every pH (Fig. 5a). The decrease of F213I mutant β-Glu activity at neutral pH was attenuated by NOV in a dose-dependent manner (Fig. 5b).

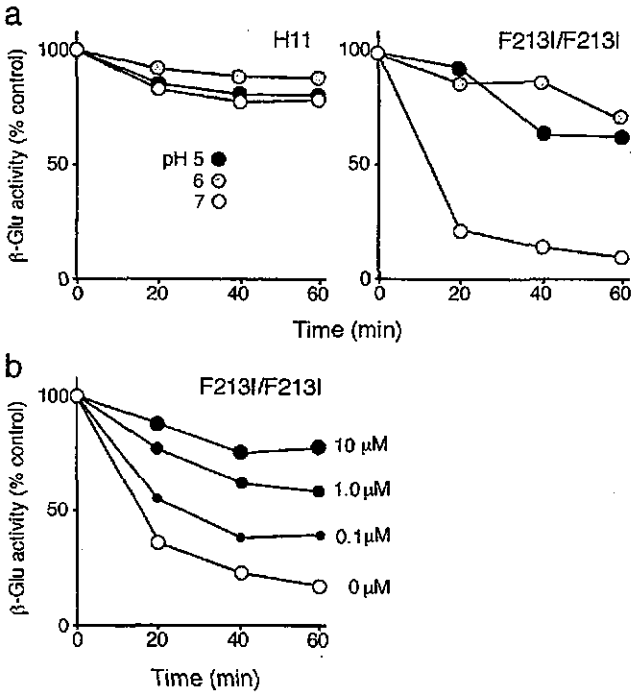


Fig. 5. Effects of NOV on pH-dependent loss of F213I mutant β-Glu activity in vitro. (a) Time course. Cell lysates were incubated at 37 °C in 0.1 M citrate-phosphate buffer at the indicated pH and the enzyme activity was determined at pH 4.5. (b) Effects of NOV. F213I/F213I cell lysates were incubated at pH 7 in the absence or presence of NOV at the concentrations indicated. Each point represents mean values of triplicate determinations obtained in a single experiment. Values were expressed as relative to the activity before the incubation (100%). Similar results were obtained in two other experiments.

## 4. Discussion

We found in the current study that, when applied to GD cells with F213I mutations, NOV up-regulated cellular β-Glu activity (Fig. 2) and accelerated cellular clearance of GlcCer (Fig. 4). NOV caused a modest but significant increase in the protein level of the mutant enzyme and increased its activity in the lysosome (Fig. 3). We also found pH-dependent loss of F213I mutant β-Glu activity in vitro and its prevention by NOV (Fig. 5). These findings are most likely explained by an activity of NOV as a chemical chaperone to accelerate transport and maturation of F213I mutant β-Glu. Although details are yet to be proven, we suppose that F213I mutant β-Glu is degraded in the ER because of its instability at neutral pH. With the aid of NOV, this mutant β-Glu is protected from degradation and is transported to the lysosome where it is stabilized because of the acidic condition and cellular enzyme activity is restored. Since effects of NOV on ER enzymes responsible for β-Glu degradation have not been examined, an alternative possibility remains to be excluded that the observed effects of NOV were secondary to inhibition of such enzyme(s). Although we have shown negative effects of NOV on some other lysosomal enzymes in vitro (Fig. 1b), potential effects of this compound on ER enzymes must be the subject of future studies.

Because NOV is an inhibitor of β-Glu ($IC_{50}$ = 3 μM, Fig. 1b), it should inhibit β-Glu activity at the lysosome if it reaches to an appropriate concentration in this compartment. NOV was most effective in inducing F213I mutant β-Glu activity at 30 μM in the medium (Fig. 2a), which was 10 times higher than its $IC_{50}$ value. NOV at this concentration, however, failed to inhibit $^{14}$C-GlcCer clearance both in control and F213I/F213I cells (Fig. 4). One possible explanation for this apparent lack of inhibition is that at 30 μM in the medium, the concentration of NOV in the lysosome did not rise high enough to inhibit β-Glu activity (whereas the concentration in the ER did rise high enough to prevent mutant β-Glu degradation). If this is the case, the action of NOV as a β-Glu inhibitor may emerge at inappropriately high concentrations. Indeed, NOV was less effective at 100 μM in increasing F213I mutant β-Glu activity (Fig. 2a), although it is yet to be proven that it was due to this action of NOV. We noticed similar dose dependence for DGJ to increase mutant α-Gal A activity in Fabry lymphocytes [10]. Thus, it is apparent that there is an appropriate concentration range for an enzyme inhibitor to up-regulate cellular enzyme activities.

The effect of NOV on cellular enzyme activity was specifically observed in GD cells with F213I mutations

but not in cells with other point mutations N370S, L444P and RecNciI (L444P and A456P) (Fig. 2a). Although a precise molecular basis is left unknown, this selectivity might depend on the differences in the stability of individual enzymes, or alternatively, on the differences of NOV-binding capacities. In this context, the lack of NOV effects on N370S/84GG cells is in contrast to the reported effects of NN-DNJ that caused a twofold increase of β-Glu activity in N370S homozygous cells [12]. It should be clarified in future studies whether this difference in the effects of NOV and NN-DNJ is due simply to the cell lines employed, or to differential binding capacities of N370S mutant enzyme to these substances.

N370S is the most common mutation in GD patients and is associated only with type 1 non-neuronopathic GD [1]. F213I is one of the two prevalent mutations in Japanese GD patients, found in 15% of alleles [19]. Clinically, patients with F213I mutations have either non-neuronopathic or neuronopathic GD. NOV may be of particular therapeutic value in the latter group, since there is no established therapy against GD brain lesions. We have shown that NOEV, an isomer of NOV, could penetrate the blood–brain barrier in mice [14]. It must be determined in a future study whether NOV penetrates the blood–brain barrier and exerts its activity on mutant β-Glu in the brain.

Finally, besides F213I, other β-Glu mutant forms are a potential target of NOV or related compounds. In this context, it should be noted that in a report of a neuronopathic GD patient with G202R mutations, ultrastructural immunohistochemistry revealed the absence of the mutant protein in the lysosome, despite its abundant presence in the ER [28]. So far, nojirimycin derivatives have been an only known class of carbohydrate mimics with chemical chaperone activity for lysosomal enzymes [10–12]. Together with NOEV [14], NOV represents a novel class of carbohydrate mimics with a potential chemical chaperone activity. It is a subject of future studies to test whether NOV and related compounds work as a chemical chaperone for other β-Glu mutant forms, and further for other mutant lysosomal enzymes.

## Acknowledgements

This work was supported in part by grant "Research on Psychiatric and Neurological disorders and Mental Health" from the ministry of Health, Labor and Welfare of Japan.

## References

[1] E. Beutler, G.A. Grabowski, Gaucher disease, The Metabolic and Molecular Bases of Inherited Disease, McGraw-Hill, New York, 2001, pp. 2641–2670.

[2] N.W. Barton, R.O. Brady, J.M. Dambrosia, A.M. Di Bisceglie, S.H. Doppelt, S.C. Hill, H.J. Mankin, G.J. Murray, R.I. Parker, C.E. Argoff, et al., Replacement therapy for inherited enzyme deficiency—macrophage-targeted glucocerebrosidase for Gaucher's disease, N. Engl. J. Med. 324 (1991) 1464–1470.

[3] D.I. Rosenthal, S.H. Doppelt, H.J. Mankin, J.M. Dambrosia, R.J. Xavier, K.A. McKusick, B.R. Rosen, J. Baker, L.T. Niklason, S.C. Hill, et al., Enzyme replacement therapy for Gaucher disease: skeletal responses to macrophage-targeted glucocerebrosidase, Pediatrics 96 (1995) 629–637.

[4] G.A. Grabowski, N. Leslie, R. Wenstrup, Enzyme therapy for Gaucher disease: the first 5 years, Blood Rev. 12 (1998) 115–133.

[5] C.A. Prows, N. Sanchez, C. Daugherty, G.A. Grabowski, Gaucher disease: enzyme therapy in the acute neuronopathic variant, Am. J. Med. Genet. 71 (1997) 16–21.

[6] R. Schiffmann, M.P. Heyes, J.M. Aerts, J.M. Dambrosia, M.C. Patterson, T. DeGraba, C.C. Parker, G.C. Zirzow, K. Oliver, G. Tedeschi, et al., Prospective study of neurological responses to treatment with macrophage-targeted glucocerebrosidase in patients with type 3 Gaucher's disease, Ann. Neurol. 42 (1997) 613–621.

[7] M. Aoki, Y. Takahashi, Y. Miwa, S. Iida, K. Sukegawa, T. Horai, T. Orii, N. Kondo, Improvement of neurological symptoms by enzyme replacement therapy for Gaucher disease type IIIb, Eur. J. Pediatr. 160 (2001) 63–64.

[8] T. Cox, R. Lachmann, C. Hollak, J. Aerts, S. van Weely, M. Hrebicek, F. Platt, T. Butters, R. Dwek, C. Moyses, et al., Novel oral treatment of Gaucher's disease with N-butyldeoxynojirimycin (OGT918) to decrease substrate biosynthesis, Lancet 355 (2000) 1481–1485.

[9] F.M. Platt, M. Jeyakumar, U. Andersson, D.A. Priestman, R.A. Dwek, T.D. Butters, Inhibition of substrate synthesis as a strategy for glycolipids lysosomal storage disease therapy, J. Inherit. Metab. Dis. 24 (2001) 275–290.

[10] J.Q. Fan, S. Ishii, N. Asano, Y. Suzuki, Accelerated transport and maturation of lysosomeal α-galactosidase A in Fabry lymphoblasts by an enzyme inhibitor, Nat. Med. 5 (1999) 112–115.

[11] L. Tominaga, Y. Ogawa, M. Taniguchi, K. Ohno, J. Matsuda, A. Oshima, Y. Suzuki, E. Nanba, Galactonojirimycin derivatives restore mutant human β-galactosidase activities expressed in fibroblasts from enzyme-deficient knockout mouse, Brain Develop. 23 (2000) 228–284.

[12] A.R. Sawkar, W.C. Cheng, E. Beutler, C.H. Wong, W.E. Balch, J.W. Kelly, Chemical chaperones increase the cellular activity of N370S β-glucosidase: a therapeutic strategy for Gaucher disease, Proc. Natl. Acad. Sci. U. S. A. 99 (2002) 15428–15433.

[13] S. Ogawa, M. Ashiura, C. Uchida, S. Watanabe, C. Yamazaki, K. Yamagishi, J. Inokuchi, Synthesis of potent β-D-glucocerebrosidase inhibitors: N-alkyl-β-valienamines, Bioorg. Med. Chem. Lett. 6 (1996) 929–932.

[14] J. Matsuda, O. Suzuki, A. Oshima, Y. Yamamoto, A. Noguchi, K. Takimoto, M. Itoh, Y. Matsuzaki, Y. Yasuda, S. Ogawa, Y. Sakata, E. Nanba, K. Higaki, Y. Ogawa, L. Tominaga, K. Ohno, H. Iwasaki, H. Watanabe, R.O. Brady, Y. Suzuki, Chemical chaperone therapy for brain pathology in G(M1)-gangliosidosis, Proc. Natl. Acad. Sci. U. S. A. (2003) 15912–15917.

[15] S. Ogawa, Y. Kobayashi, K. Kabayama, M. Jimbo, J. Inokuchi, Chemical modification of β-glucocerebrosidase inhibitor N-octyl-β-valienamine: synthesis and biological evaluation of N-alkanoyl and N-alkyl derivatives, Bioorg. Med. Chem. 6 (1998) 1955–1962.

[16] H. Lin, K. Ohno, Preclinical research of a new therapy for Gaucher's disease with F213I mutation, Zhonghua YiXue YiChuan Xue ZaZhi 20 (2003) 381–384.

[17] E.I. Ginns, F.P. Tegelaers, R. Barneveld, H. Galjaard, A.J. Reuser, R.O. Brady, J.M. Tager, J.A. Barranger, Determination of Gaucher's disease phenotypes with monoclonal antibody, Clin. Chim. Acta 131 (1983) 283–287.

[18] S. Ichisaka, K. Ohno, I. Yuasa, E. Nanba, H. Sakuraba, Y. Suzuki, Increased expression of β-hexosaminidase α chain in cultured skin fibroblasts from patients with carbohydrate-deficient glycoprotein syndrome type I, Brain Develop. 20 (1998) 302–306.

[19] Y. Eto, H. Ida, Clinical and molecular characteristics of Japanese Gaucher disease, Neurochem. Res. 24 (1999) 207–211.
[20] A.M. Vaccaro, M. Muscillo, M. Tatti, R. Salvioli, E. Gallozzi, K. Suzuki, Effect of a heat-stable factor in human placenta on glucosylceramidase, glucosylsphingosine glucosyl hydrolase, and acid β-glucosidase activities, Clin. Biochem. 20 (1987) 429–433.
[21] Y. Suzuki, A. Tsuji, K. Omura, G. Nakamura, S. Awa, M. Kroos, A.J. Reuser, Km mutant of acid α-glucosidase in a case of cardiomyopathy without signs of skeletal muscle involvement, Clin. Genet. 33 (1988) 376–385.
[22] Y. Sugimoto, H. Ninomiya, Y. Ohsaki, K. Higaki, J.P. Davies, Y.A. Ioannou, K. Ohno, Accumulation of cholera toxin and GM1 ganglioside in the early endosome of Niemann–Pick C1-deficient cells, Proc. Natl. Acad. Sci. U. S. A. 98 (2001) 12391–12396.
[23] L.S. Chin, M.C. Raynor, X. Wei, H.Q. Chen, L. Li, Hrs interacts with sorting nexin 1 and regulates degradation of epidermal growth factor receptor, J. Biol. Chem. 276 (2001) 7069–7078.
[24] A. Klein, M. Henseler, C. Klein, K. Suzuki, K. Harzer, K. Sandhoff, Sphingolipid activator protein D (sap-D) stimulat ɔsomal degradation of ceramide in vivo, Biochem. Biophy mmun. 200 (1994) 1440–1448.
[25] Y. Liu, Y.P. Wu, R. Wada, E.B. Neufeld, K.A. Mul oward, P.G. Pentchev, M.T. Vanier, K. Suzuki, R.L. Pro tion of neuronal ganglioside storage does not improve the urse of the Niemann–Pick C disease mouse, Hum. Mol (2000) 1087–1092.
[26] M. Pasmanik-Chor, L. Madar-Shapiro, E.O. Stein, S. Gatt, M. Horowitz, Expression of mutated glucocereb leles in human cells, Hum. Mol. Genet. 6 (1997) 887–895.
[27] Y. Oda, N. Hosokawa, I. Wada, K. Nagata, EDEM as an acceptor of terminally misfolded glycoproteins released from calnexin, Science 299 (2003) 1394–1397.
[28] K.P. Zimmer, P. le Coutre, H.M. Aerts, K. Harzer, M. Fukuda, J.S. O'Brien, H.Y. Naim, Intracellular transport of acid β-glucosidase and lysosome-associated membrane proteins is affected in Gaucher's disease (G202R mutation), J. Pathol. 188 (1999) 407–414.

Available online at www.sciencedirect.com

SCIENCE DIRECT

Brain Research 1022 (2004) 244–246

BRAIN RESEARCH

www.elsevier.com/locate/brainres

Short communication

# Degeneration of cholecystokinin-immunoreactive afferents to the VPL thalamus in a mouse model of Niemann-Pick disease type C

Shinji Ohara[a,*], Yoko Ukita[b], Haruaki Ninomiya[c], Kousaku Ohno[d]

[a]*Department of Neurology, National Chushin-Matsumoto Hospital, 811 Kotobuki, Matsumoto 399-0021, Japan*
[b]*Riken Harima Institute, Sayo, Hyogo, Japan*
[c]*Department of Neurobiology, Tottori University School of Medicine, Yonago, Japan*
[d]*Department of Child Neurology, Tottori University School of Medicine, Yonago, Japan*

Accepted 15 June 2004

**Abstract**

*Niemann-Pick* disease type C (NP-C) is a progressive neurological disorder of lipid metabolism. The Balb/C npc1 mutant strain is a genetically authentic murine model of NPC, which reproduce the clinical and histologic features of human NP-C. In the present study, we show that cholecystokinin (CCK)-immunoreactive fibers in the thalamic VPL nuclei, which are densely distributed in controls, degenerate in NPC mice. This degeneration is associated with the appearance of CCK-immunoreactive axonal spheroids containing characteristic intracellular inclusions of NP-C. These observations provide supportive evidence of the occurrence of dying-back axonopathy of neurons in the dorsal column nuclei in this mouse model.


*Theme:* Neurotransmitters, modulators, transporters and receptors
*Topic:* Peptides: anatomy and physiology

*Keywords:* Niemann-Pick type C; Cholecystokinin; VPL thalamus; Axonal spheroid

Niemann-Pick disease type C (NP-C) is an autosomal recessive disorder of lipid storage metabolism. Neuropathologically, it is characterized by the widespread appearance of axonal spheroids, an accumulation of intraneuronal cytoplasmic inclusions, and neuronal loss [2,13]. A Balb/C-npc1 mutant strain is a genetically authentic murine model of NP-C, and homozygous mice show progressive weight loss and tremor/ataxia until death at 12–14 weeks of age [9,10]. The sensory thalamus is one of the most vulnerable in this mouse model with neuronal loss beginning as early as 4 weeks of age; its degeneration may be responsible for the early appearance of motor incordination in these animals [15]. Although the mechanism of neurodegeneration in NP-C is currently unknown, the apparent topographical differences in terms of neuronal vulnerability may reflect the differential role played by NP-C1 protein in a particular neuronal population.

Cholecystokinin (CCK) is the most ubiquitous neuropeptide in the central nervous system. In sensory nervous system of both humans and rodents, CCK localizes in the dorsal root ganglia and is known to be upregulated in case involving peripheral nerve injury including nerve transection [3,14]. The appearance of CCK-immunoreactive axonal spheroids has been described in aging rat gracile nuclei [8]. CCK mRNA is also found in the sensory neurons of the dorsal column nuclei of the medulla oblongata [1]. Recent studies have demonstrated that CCK-immunoreactive fibers are present in the VPL thalamus and that the source of their immunoreactivity could be ascribed to the ipsilateral gracile nuclei, suggesting that CCK plays an important role in modulating the gracile-VPL thalamus sensory pathway [1,4].

* Corresponding author. Tel.: +81 263 58 3121; fax: +81 263 86 3190.
*E-mail address:* neuro@cameo.plala.or.jp (S. Ohara).

0006-8993/$ - see front matter © 2004 Elsevier B.V. All rights reserved.
doi:10.1016/j.brainres.2004.06.037

We recently reported that in Balb/c npc1 mice, an authentic animal model of NP-C, the neurons of the VPL/VPM thalamus started to degenerate as early as 5 weeks of age, indicating one of the most vulnerable sites in the CNS in terms of neuronal loss [15]. The VPL thalamus receives afferents from the dorsal column nuclei in the medulla oblongata, and also receives diffuse afferents from the cerebral cortices. It is still unknown whether this process accompanies or precedes the degeneration of the presynaptic terminals of the fibers projecting from the gracile nuclei. In this study, we employed CCK-immunohistochemical analysis to investigate the alteration of afferent terminals of the fibers projecting from the gracile nucleus. We found that CCK-immunoreactive fibers in the VPL thalamus of NP-C mice underwent progressive degeneration associated with the formation of axonal spheroids.

A colony of Balb/c npc$^{nih}$ mutant mice has been maintained and the genotype of each mouse was determined by PCR using genomic DNA isolated from a small piece of the tail, as previously described [6]. Affected mice of 3, 6, and 9 weeks of age ($n \geq 4$ each) and age-matched control mice ($n=3$) were used in this study. Animals were anesthetized using sodium pentobarbital solution (Dinabot) and were perfused transcardially with heparinized PBS followed by freshly prepared 4% paraformaldehyde in 0.1M phosphate buffer. For the electronmicroscopic study, glutaraldehyde was added to the perfusion fixative to a concentration of 0.5%. The brain and the spinal cord were resected and postfixed overnight in the same fixative. The coronal slices of the brain were cut to obtain tissue blocks of the VPL/VPM thalamus. The sections were paraffin-embedded and stained with H and E, cresyl-violet and PAS. Immunohistochemistry was performed using streptoavitin biotin methods with the following primary antibody: rabbit polyclonal CCK (1:10,000; the kind gift of Dr. Tramu, University of Bordeaux), GFAP (1:500 DAKO, Stockholm, Sweden). The reaction products were visualized by the avitin–biotin method (Vecstastain ABC kit, Vector lab., Burlingame, CA). For the electronmicroscopy, tissue blocks were post-fixed with 1% osmium tetroxide, dehydrated in a graded ethanol series, and then were embedded in Epon 812 (Polyscience, Warrington, PA). One-micrometer-thick sections were cut and stained with 1% toluidine blue, and ultrathin sections from selected blocks were cut and stained with uranyl acetate and lead citrate. The sections were examined under a Joel 1200 electron microscope. For the ultrastructural CCK-immunohistochemisry, 9-week-old NP-C mice ($n=3$) were perfused with 4% paraformaldehyde. Forty-micrometer-thick sections were cut on a vibratome and were immunostained using the same protocol as that used for the LM sections, and then the sections were processed for electron microscopy.

CCK-immunohistochemistry revealed abundant positive fibrils in the control VPL nuclei (Fig. 1A). The distribution of positive fibrils was in accordance with those reported by Hunt et al. in rat VPL nuclei. The fibrils appeared in bundles or in dots (Fig. 1B). In the NP-C mice, essentially the same bundle-like staining pattern could still be recognized at 3 and 6 weeks. At 9 weeks, fragmentation of the CCK-immunoreactive fibrils was evident in the VPL thalamus, as was a decrease in the number of these fibrils (Fig. 1B,D). The overall size of the spheroids increased at 9 weeks, compared to that at 3 and 6 weeks, and some of the spheroids exhibited CCK-immunoreactivity at the peripheral rim (Fig. 1F).

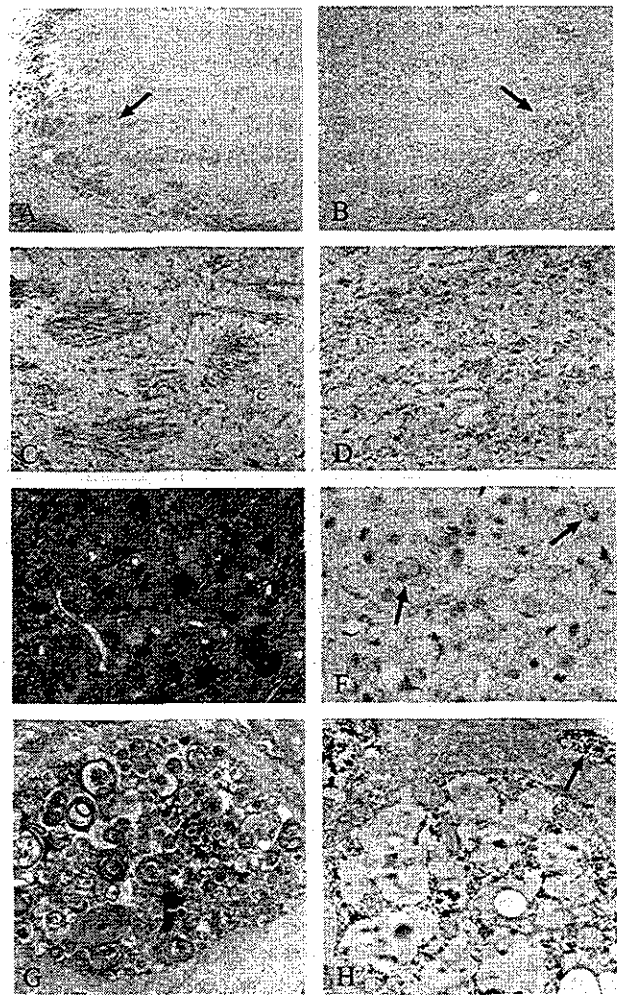


Fig. 1. (A and B) CCK-immunoreactive fibers in the thalamus of BALB/c control (A) and NP-C (B) mice at 9 weeks. The arrows indicate the location of the VPL nucleus. (×27) (C and D) Higher magnification of the area in the VPL nuclei indicated by the arrows in A (for C) and B (for D). In the controls, the CCK-immunoreactive fibers appeared in bundles, whereas in the NP-C mice, the disintegration of CCK-immunoreactive fibers is evident. (×180) (E) Epon semi-thin section of the VPL nucleus of an NP-C mouse at 9 weeks. Note the many spheroids (arrowheads) with up to 14 μm in diameter. (×320) (F) CCK-immunohistochemistry of the VPL nucleus of NP-C mouse at 9 weeks. The arrows indicate peripheral CCK-immunostaining of axonal spheroids. (×320) (G) Electron microscopy of axonal spheroids revealing the massive accumulation of lamellated inclusions. (×4400) (F) CCK-immunoelectron microscopy. CCK-immunoreactivity was observed in the neural process (arrow) and in axonal spheroids, excluding intracytoplasmic inclusions. (×9900).

Immunostaining with anti-ubiquitin antibody revealed that many of the spheroids were ubiquitin-immunoreactive.

Epon semi-thin sections showed no neuronal loss in the VPL nuclei at 3 weeks and only a few axonal spheroids were observed. At 6 weeks, a loss of neurons and the appearance of hypertrophic astrocytes were evident in the nuclei. The axonal spheroids increased in both number and size. At 9 weeks, the nuclei revealed massive appearance of axonal spheroids, in addition to a nearly complete loss of neurons (Fig. 1E).

Electron microscopy revealed that the spheroids contained numerous lamellated inclusions characteristic of NP-C (Fig. 1G). CCK-immunoreactivity was ultrastructurally localized in the cell processes and cytoplasm of the spheroids surrounding the inclusions (Fig. 1H). In the gracile nuclei, the appearance of dystrophic axons with characteristic ultrastructural features, e.g., tubulovesicular profiles, was evident at 6 weeks [9]; in the present study, however, no dystrophic features were recognized in the VPL thalamus at 9 weeks.

By experimentally lesioning the dorsal column nuclei and by conducting tracer studies in combination with immunohistochemistry, previous reports have convincingly shown that the major source of CCK-immunoreactive fibers is the dorsal column nuclei in the medulla oblongata [1,4]. The present immunohistochemical study confirmed the presence of CCK-immunoreactive fibers in the VPL thalamic nuclei in Balb/c mice, which was first demonstrated in rats [4].

In NP-C mice, we have shown a reduction and disintegration of CCK-immunoreactive fibers in the VPL thalamic nuclei, both of which were most evident at 9 weeks. These findings were associated with the appearance of CCK-immunoreactive axonal spheroids, strongly suggesting an occurrence of axonopathy involving the afferent terminals of gracile neurons in this NP-C mouse model. Axonal spheroid formation (swelling) has been regarded as one of the cardinal histological features of the NP-C brain [2,13]. However, the ultrastructure of axonal spheroids in various locations in the NP-C brain has not been systematically studied. Our recent study demonstrated that in this model mice, ultrastructurally defined dystrophic changes develop prematurely in the presynaptic axon terminals of DRG neurons in the dorsal column nuclei and spinal dorsal horn [11]. In the present ultrastructural study, no such dystrophic features were recognized in the CCK-immunoreactive spheroids in the VPL thalamus. This morphological difference of axonal spheroids between the two nuclei may reflect an inherent tendency of the dorsal column nuclei to develop axonal dystrophy as a function of age [5]. At present, the significance of axonal spheroid formation in neuronal degeneration is not entirely clear. However, recent studies have demonstrated that the degeneration of axons precedes that of neuronal cell body, suggesting the occurrence of dying-back axonopathy in NP-C [7,11,12]. Our observation made on the VPL thamalus provides supportive evidence of the occurrence of dying-back type degeneration in the dorsal column neurons in this mouse model of NP-C.

## Acknowledgement

We are grateful to Mr. N. Takeda, Department of Clinical Laboratory Research, National Chushin-Matsumoto Hospital, for his technical assistance.

## References

[1] S. Farnebo, O. Hermanson, A. Blomqvist, Thalamic-projecting preprocholecystokinin messenger RNA-expressing neurons in the dorsal column nuclei of the cat, Neuroscience 78 (1997) 1051–1057.
[2] Y. Higashi, P.G. Pentchev, S. Murayama, K. Suzuki, Pathology of Niemann-Pick type C: Studies of murine mutants, in: F. Ikuta (Ed.), Neuropathology in Brain Research, Elsevier, 1991, pp. 85–102.
[3] T. Hokfelt, R. Cortes, M. Schalling, S. Ceccatelli, M. Pelto-Huikko, H. Persson, M.J. Villar, Distribution pattern of CCK and CCK mRNA in some neuronal and non-neuronal tissues, Neuropeptides 19 (1991) 31–43.
[4] C.A. Hunt, K.B. Seroogy, C.M. Gall, E.G. Jones, Cholecystokinin innervation of rat thalamus, including fibers to ventroposterolateral nucleus from dorsal column nuclei, Brain Res. 426 (1987) 257–269.
[5] K. Jellinger, Neuroaxonal dystrophy: its natural history and related disorders, Prog. Neuropathol. 2 (1973) 129–180.
[6] S.K. Loftus, J.A. Morris, E.D. Carstea, J.Z. Gu, C. Cummings, A. Brown, J. Ellison, K. Ohno, M.A. Rosenfeld, D.A. Tagle, P.G. Pentchev, W.J. Pavan, Murine model of Niemann-Pick C disease: mutation in a cholesterol homeostasis gene, Science 277 (1997) 232–235.
[7] P.A. March, M.A. Thrall, D.E. Brown, T.W. Mitchell, A.C. Lowenthal, S.U. Walkley, GABAergic neuroaxonal dystrophy and other cytopathological alterations in feline iemann-Pick disease type C, Acta Neuropathol. 94 (1997) 164–172.
[8] T. Matusda, M. Maeda, Y. Morishima, et al., Dystrophic axons in the nucleus gracilis of the normal rat containing cholecystokinin-like immunoreactivity, Acta Neuropathologica 65 (1985) 224–234.
[9] S. Miyawaki, S. Mitsuoka, T. Sakiyama, T. Kitagawa, Sphingomyelinosis, a new mutation in the mouse, J. Hered. 73 (1982) 257–263.
[10] M.D. Morris, C. Bhuvaneswaren, H. Shio, S. Fowker, Lysosomal lipid storage disorder in NCTR-BALB/c mice, Am. J. Pathol. 108 (1982) 140–149.
[11] S. Ohara, Y. Ukita, H. Ninomiya, K. Ohno, Axonal dystrophy of dorsal root ganglion sensory neurons in a mouse model of Niemann-Pick disease type C, Exp. Neurol. 187 (2004) 289–298.
[12] W.-Y. Ong, U. Kumar, R.C. Switzer, A. Sidhu, G. Suresh, C.-Y. Hu, S.C. Patel, Neurodegeneration in Niemann-Pick type C disease mice, Exp. Brain Res. 141 (2001) 218–231.
[13] M.T. Vanier, K. Suzuki, Recent advances in elucidating Niemann-Pick disease, Brain Pathol. 8 (1998) 163–174.
[14] X.-J. Xu, M.J.C. Puke, V.M.K. Verge, Z. Wiesenfeld-Hallin, J. Hughes, T. Hokfelt, Up-regulation of cholecystokinin in primary sensory neurons is associated with morphine insensitivity in experimental neuropathic pain in the rat, Neurosci. Lett. 152 (1993) 129–132.
[15] A. Yamada, M. Saji, Y. Ukita, Y. Shinoda, M. Taniguchi, K. Higaki, H. Ninomiya, K. Ohno, Progressive neuronal loss in the ventral posterior lateral and medial nuclei of thalamus in Niemann-Pick disease type C mouse brain, Brain Develop. 23 (2001) 288–297.

# たけのこ

2004.1.20 発行

目 次


■ 代表あいさつ……1
■ 本部総会報告……2
■ 本部総会を終えて……3
■ 支部報告……4
■ 特　　集……10
■ こえのひろば……19
■ 掲 示 板……27



竹の子の会
プラダー・ウィリー症候群親の会

第23号